OPTIMIZATION OF PARAMETERS TO MINIMIZE THE SKIN FRICTION COEFFICIENT IN ABRASIVE WATER SUSPENSION JET MACHINING THROUGH TLBO

Rakesh Kumar Sahu[1],Saurabh Verma[2],Santosh Kumar Mishra [3]
[1, 2 ,3]Department of Mechanical Engineering
Bhilai Institute of Technology,Durg, India
Email:[1]rakeshkumarsahu10@rediffmail.com, [2]san810@gmail.com,

Abstract
Abrasive water suspension jet (AWSJ) machining is material removal process where the material is removed by high velocity stream of water and abrasive mixture. Abrasive particles moving with the flow cause severe skin friction effect which reduces the life of nozzle for effective machining. In the present work, According to the structure of nozzle computational domain has been modeled using commercially available pre-processor routine called GAMBIT, and CFD Analysis has been performed in ANSYS (fluent) to obtain the values of SFC for different values of parameters. Based on the Analysis at the critical section of nozzle an empirical formula has been developed for SFC. TLBO algorithm has been used to optimize the parameters to minimize the SFC in AWSJ machining. To validate the result CFD Analysis has been performed to obtain the value of SFC for optimized value of parameters.

Key Words: Abrasive water suspension jet (AWSJ) machining, nozzle geometry, nozzle wear, fluid flow, MRR, Erosion rate, Teaching-Learning-Based Optimization (TLBO).

Broad Area - Mechanical Engineering.

Sub-Area - Fluid Mechanics.

1. Introduction

Abrasive water suspension jet (AWSJ) machining is a well-established non-traditional machining process which uses the principles of both abrasive jet machining and water jet machining. AWSJ machining is a non-conventional machining process where material is removed by impact erosion of high pressure high velocity of water and entrained high velocity of grit abrasives on a work piece [8]. In abrasive water suspension jet machining process pure water (tap water) is used and for abrasive particles like sand (SiO_2), glass beads, Aluminum oxide, and silicon carbide is generally used. In AWSJ machining in which suspended abrasive particles in liquid medium called slurry is pressurized and expelled through the nozzle. Slurry is accelerated through a fine orifice to produce a high velocity stream, which is capable of machining a range of materials [2]. The rapid advances in AWSJ machining is due to high capability of the process to machine complex shapes that need to be produced from brittle and heat sensitive materials and also from the need to machine different variety of composites. One of the plaguing problems faced by AWSJ machining is nozzle wear mainly due to the suspension particles in the jet [27]. M. Hashish et al [2] experimentally investigated observations of wear of abrasive-waterjet nozzle materials and found that Tube made with tough section at the entry and a hard section at the exit has an improved wear performance. M. Nanduri et al [6] analyzed experimentally nozzle wear in abrasive waterjet machining process. The result founded in this paper is that the effect of nozzle length, inlet angle, diameter, orifice diameter, abrasive flow rate, and water pressure on nozzle wear was studied and the nozzle wear model was

developed for prediction the wear. J. john et al. [10] has done experimental work and gave strategy for the efficient and quality cutting of materials and suggest that to achieve higher efficiency and desired quality, it is required to monitor the condition of nozzles and considering the change in the dimension of orifice and focusing nozzle.

H. Liu et al. [9] carried out Computational Fluid Dynamic (CFD) analysis to study the jet dynamic characteristics of flow downstream. Kyriaki et al. [11] proposed a finite element-based model for pure waterjet process simulation and the main objective was to investigate and analyzed in detail the work piece material behavior under waterjet impingement; a non-linear FE model (using LS-DYNA 3D code) had been developed which simulates the erosion of the target material caused by the high pressure waterjet flow. The simulation model can provide a lot of results to the user and it can be useful in studying the overall waterjet process and for the optimization of the waterjet parameters. Deepak D et al. [20] analyzed the effect of inlet operating pressure on skin friction coefficient and jet exit kinetic energy in single step nozzle. It is found that an increase in inlet operating pressure causes a significant increase in skin friction coefficient and also results in proportional increase in the exit kinetic energy of the jet.

Rao et al. [23] proposed a new efficient optimization method, called 'Teaching–Learning-Based Optimization (TLBO)', for the optimization of mechanical design problems. This method works on the effect of influence of a teacher on learners. Pawar et al. [24] presented TLBO algorithm to find the optimal combination of process parameters for the considered machining processes. It was observed that TLBO algorithm is slightly better in terms of accuracy of solution. Rao & patel (2012a) proposed an elitist teaching learning based optimization algorithm for solving complex constrained optimization problems. The results show that elitism consideration produces better results than without elitism consideration.

Nomenclature

d Focus tube diameter (mm)
dp Diameter of abrasive particles (μm)
D Inlet diameter of nozzle (mm)
FLift Lift force (N)
Fs External body force (N)
Fvm Virtual mass force (N)
K Momentum exchange co-efficient
l Length of flow domain (mm)
L Particle spacing (mm)
m Mass flow rate of mixture (m3/s)
St Stokes number
ts system response time (s)
V Velocity of phase (m/s)
α Volume fraction of the phase
β Particulate loading
ρ Density of suspension mixture (kg/m3)
γ Density ratio
τd Particle response time (s)
μ Viscosity (kg/m-s)
Subscripts
p, q phases
l liquid phase
s solid phase

2. Theoretical formulation

2.1 Numerical Model and Assumptions

The numerical region for flow analysis is made up of flow geometry given in the Fig. 1 for the single step AWSJ nozzle. Computational domain consists of converging nozzle of diameter 4mm, nozzle length 4mm straight duct is introduced. There is a focus tube of diameter 1.3mm and length 17mm. The Abrasive water suspension mixture is let into the nozzle at the inlet and is carried down through the converging cone to the focus tube and exits as coherent jet at the nozzle exit, in which the focus tube is used for stabilizing the flow.

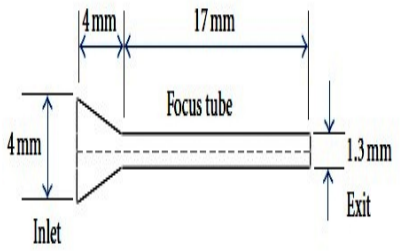

Fig.1: Computational domain of single step nozzle according to Deepak et al. [20].

The numerical model adopted closely follows the work of G.Hu et al [4] in which liquid solid two-phase flow is considered and the following assumptions are valid for the present work.

I. The primary liquid phase is continuous and incompressible.

II. Flow is taken to be two-phase flow in which the primary liquid phase mixes homogeneously with the particles of equal diameter, constituting the solid phase.

III. Two-phase flow assumed is steady and characterized by turbulent flow.

2.2 The computation of particulate loading and stokes number

Particulate loading and the stokes number are important parameters that help to identify the appropriate multiphase model. Particulate loading has a major impact on phase interactions and is defined as the mass density ratio of the dispersed phase to that of the carrier phase.

The particulate loading for garnet abrasive is

$$\beta = \frac{\alpha_s \rho_s}{\alpha_l \rho_l} = \frac{0.1x2300}{998} = 0.230 \quad (1)$$

For silicon carbide abrasive is

$$\beta = \frac{\alpha_s \rho_s}{\alpha_l \rho_l} = \frac{0.1x3170}{998} = 0.318 \quad (2)$$

For aluminum oxide abrasive is

$$\beta = \frac{\alpha_s \rho_s}{\alpha_l \rho_l} = \frac{0.1x2719}{998} = 0.27 \quad (3)$$

The degree of interaction between the phases is intermediate loading, the coupling is two-way i.e., the fluid carrier influences the particulate phase via drag and turbulence, but the particles in turn influence the carrier fluid via reduction in mean momentum and turbulence. All multiphase models can handle this type of problem but it is found that the Eulerian multiphase model seems to be the most accurate one. The average distance between the individual particles of the particulate phase can be estimated by equation developed by Crowe et al (2009).

For garnet abrasive:

$$\gamma = \frac{\rho_s}{\rho_l} = \frac{2300}{998} = 2.3 \quad (4)$$

$$k = \frac{\beta}{\gamma} = \frac{0.230}{2.30} = 0.100 \quad (5)$$

$$\frac{L}{d_p} = \left(\frac{\pi}{6}\frac{1+k}{k}\right)^{\frac{1}{3}} = \left(\frac{\pi}{6}\frac{1+0.10}{0.10}\right)^{\frac{1}{3}} = 1.7925 \quad (6)$$

The average distance between the individual particles (particle size d_p=63μm) of the particulate phase is

L=1.7925×d_p = 1.7925×0.063 = 0.1129mm

Estimating the value of the stokes number helps to select the most appropriate multiphase model. The stokes number is defined as the ratio of the particle response time to the system response time is calculated below.

$$\tau_d = \frac{\rho_d d^2 p}{18\mu_l} = \frac{2300x\left(63x10^{-6}\right)^2}{18x0.001004} = 5.05123x10^{-4} \quad (7)$$

$$t_s = \frac{l}{v} = \frac{0.0364}{25.6} = 1.4218x10^{-3} \quad (8)$$

$$S_t = \frac{\tau_d}{t_s} = \frac{5.05129x10^{-4}}{1.4218x10^{-3}} = 0.3552 \quad (9)$$

For silicon carbide abrasive:

$$\gamma = \frac{\rho_s}{\rho_l} = \frac{3170}{998} = 3.18 \quad (10)$$

$$k = \frac{\beta}{\gamma} = \frac{0.318}{3.18} = 0.1 \quad (11)$$

L = 1.7925×0.063 = 0.1129mm

$$\tau_d = \frac{\rho_d d^2 p}{18\mu_l} = \frac{3170x(63x10^{-6})^2}{18x0.001004} = 6.96200x10^{-4} \quad (12)$$

$$t_s = \frac{l}{v} = \frac{0.0364}{25.6} = 1.4218x10^{-3} \quad (13)$$

$$S_t = \frac{\tau_d}{t_s} = \frac{5.05129x10^{-4}}{1.4218x10^{-3}} = 0.3551 \quad (14)$$

For Aluminum oxide abrasive:

$$\gamma = \frac{\rho_s}{\rho_l} = \frac{2719}{998} = 2.72 \quad (15)$$

$$k = \frac{\beta}{\gamma} = \frac{0.272}{2.72} = 0.1 \quad (16)$$

$$\frac{L}{d_p} = \left(\frac{\pi}{6}\frac{1+k}{k}\right)^{\frac{1}{3}} = \left(\frac{\pi}{6}\frac{1+0.1}{0.1}\right)^{\frac{1}{3}} = 1.7925 \quad (17)$$

L = 1.7925×0.063 = 0.1129mm

$$\tau_d = \frac{\rho_d d^2 p}{18\mu_l} = \frac{2719x\left(63x10^{-6}\right)^2}{18x0.001004} = 5.97151x10^{-4} \quad (18)$$

$$t_s = \frac{l}{v} = \frac{0.0364}{25.6} = 1.4218x10^{-3} \quad (19)$$

$$S_t = \frac{\tau_d}{t_s} = \frac{5.05129x10^{-4}}{1.4218x10^{-3}} = 0.3552 \quad (20)$$

For Stokes number less than unity, particles will closely follow the fluid flow and any one of the

three multiphase models namely Volume of fluid model, Mixture model or Eulerian multiphase model is applicable. Also from the calculation of the effect of particulate loading it is clear that coupling between two phases is intermediate. Hence present numerical simulation is carried using Eulerian multiphase model which through is most expensive in computation, but gives most accurate results. Eulerian Multiphase model is embedded in fluent software. Fluent solves a multi-fluid granular model to describe the flow behavior of fluid solid mixture. The stresses induced in the solid phase are deduced through an analogy between the random particle motion arising from particle to particle collisions and the thermal gradient of molecules in the fluid stream taking into effect the inelasticity of the granular phase. Intensity of the particle velocity fluctuations determines the stresses, viscosity and pressure of the solid phase.

The governing equations for mass and momentum conservation are solved for the steady incompressible flow. The coupling between velocity and pressure has been attempted through the phase couples SIMPLE algorithm developed by Patankar S.V. using the power law scheme for the solution. The turbulence is modeled using Realizable k-€ turbulence model. The governing partial differential equations, for mass and momentum conservations are detailed below.

Continuity Equation:

$$\frac{1}{\rho_{pq}}\left[\frac{\partial}{\partial t}(a_q\rho_q) + \nabla^{\circ}(\alpha_q\rho_q v_q)\right] = \sum_{p=1}^{N}(m_{pq} - m_{qp}) \quad (21)$$

Where p,q phases, α_q= vol.fraction of the secondary phase, ρ_{pq}= density of suspended mixture(kg/m^3), v= velocity, m= mass flow rate, N= lift force

Fluid-solid Momentum Equation:

The conservation of momentum equation for the solid phase is as follows:

$$\frac{\partial}{\partial t}(a_s\rho_s v_s) + \nabla(\alpha_s\rho_s v_s^2) = -\alpha_s\nabla \mathrm{p} - \nabla \mathrm{p_s} + \nabla^{\circ}\tau_s + a_s\rho_s g + \sum_{l=1}^{N}[k_{ls}(v_l - v_s) + (m_{ls}v_{ls} - m_{sl}v_{sl})] + \left(F_s + F_{lift,s} + F_{vm,s}\right) \quad (22)$$

Where α_s=vol. fraction of solid phase, ρ_s= density of the solid phase, v_s=velocity of the solid phase, τ_s= particle response time, l= length of flow domain (mm), F_s=external body force, $F_{vm,s}$=virtual mass force of solid phase, F_{lift}= lift force of solid phase, m = mass flow rate, K= momentum exchange coefficient

The conservation of momentum equation for the fluid phase is as follows.

$$\frac{\partial}{\partial t}(a_q\rho_q v_q) + \nabla(\alpha_q\rho_q v_q^2) = -\alpha_q\nabla \mathrm{p} + \nabla^{\circ}\tau_q + a_q\rho_q g + \sum_{l=1}^{N}[k_{pq}(v_p - v_q) + (m_{pq}v_{pq} - m_{qp}v_{qp})] + \left(F_q + F_{lift,q} + F_{vm,q}\right) \quad (23)$$

2.3 Numerical Scheme

Computational domain is modeled using commercially available pre-processor routine called GAMBIT, and meshing is carried out using grid cells of 30000 control volumes. According to the structure of nozzle computational domain is built axi-symmetric model shown in figure 2.

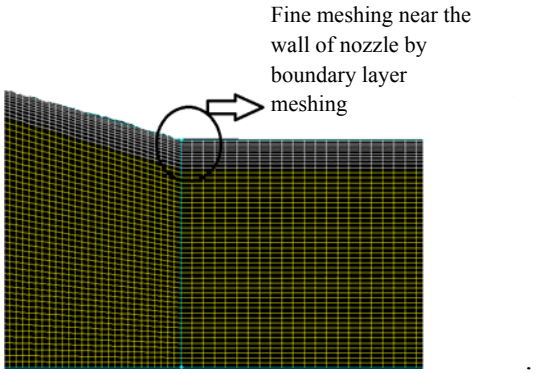

Fig. 2 A meshed domains near the wall of nozzle

2.4 Boundary Condition and Operating Parameters

Suitable boundary conditions are imposed on the computational domain, as per the physics of the problem. Inlet boundary condition is specified by the operating pressure entering the nozzle. It is assumed that velocity at inlet is uniform across the cross section. At the exit, static pressure of refluxing flow is taken to be zero (gauge), so that the computation would proceed by the relative pressure difference across the grid volumes for the entire domain of the flow. Wall boundary conditions are impressed to bound fluid and solid regions. In viscous flow models, as in the present case velocity components at the wall are

set to zero in according with the no-slip and impermeability conditions that exist on the wall boundary. The axis of the nozzle is used to solve the computational domain as axis-symmetric problem and suitable boundary conditions are imposed for the same i.e., the gradient of fluid properties are set to zero across the axis line. In the present numerical simulation suspended liquid is treated as primary phase and abrasive is treated as secondary phase.

2.5 Validation of the Numerical Model

The present model is benchmarked against the numerical work according to Deepak et al. (2012) cited in [20]. The graph of the velocity distribution of one of the phases (liquid phase) has been calibrated in the present work as shown in Fig.4 with that of the work cited in the literature according to Deepak et al. (2012) as shown in Fig.3. According to fig.3 and fig.4 in both figure Velocity magnitude first increases length along the nozzle then the velocity is constant. It is clear that there is good agreement between the two models as regards to the velocity distribution.

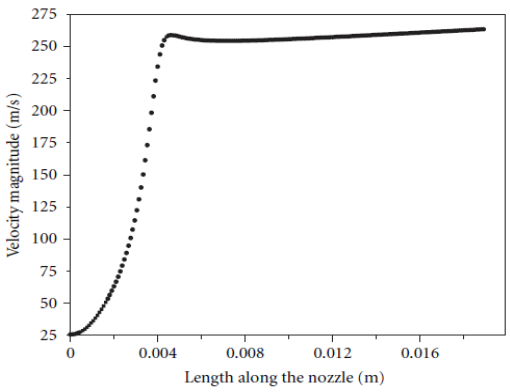

Fig. 3: The velocity distribution along the length of the single step nozzle as given in reference literature [20].

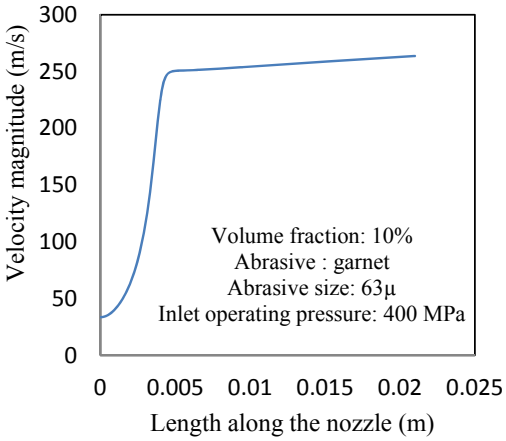

Fig. 4: The velocity distribution along the length of the single step nozzle as per the present model.

3. Method of solution

3.1 CFD Analysis of nozzle for different geometry models

CFD Analysis has performed in ANSYS (fluent) 14.0 to obtain values of SFC for various sets of parameters (Table 2). Range has been selected as given in Table 1.

Table 1

Parameters	Range	Units	Typical values
P (Inlet Operating Pressure)	100- 400	Bar	400
D (Nozzle diameter)	3.50 - 4.50	mm	4.2
d (orifice diameter)	1 -1.5	mm	1.0
ρ (density of Abrasive Particle)	2300-3170	kg/m^3	2300
L (focus length)	17-18.2	Mm	17.0

Table 2

P (Bar)	D (mm)	d (mm)	ρ (kg/m^3)	L (mm)	SFC
100	4.2	1.00	2300	17.0	0.0012314
200	4.2	1.00	2300	17.0	0.0023365
300	4.2	1.00	2300	17.0	0.0033984
400	4.2	1.00	2300	17.0	0.0044333
400	3.5	1.00	2300	17.0	0.0041870
400	3.8	1.00	2300	17.0	0.0043370
400	4.2	1.00	2300	17.0	0.0045268
400	4.5	1.00	2300	17.0	0.0046625
400	4.2	1.00	2300	17.0	0.0044333
400	4.2	1.25	2300	17.0	0.0040493
400	4.2	1.35	2300	17.0	0.0039247
400	4.2	1.50	2300	17.0	0.0037604
400	4.2	1.00	2300	17.0	0.0044333

400	4.2	1.00	2600	17.0	0.0042512
400	4.2	1.00	2900	17.0	0.0040954
400	4.2	1.00	3170	17.0	0.0039726
400	4.2	1.00	2300	17.0	0.0044333
400	4.2	1.00	2300	17.5	0.0043477
400	4.2	1.00	2300	18.0	0.0042657
400	4.2	1.00	2300	18.2	0.0041870

3.2 Based on the Analysis development of Empirical Relation for nozzle geometry

Based on the Analysis at the critical section of nozzle an empirical formula developed for the Range as given in Table 1.

$$\textbf{Skin friction coefficient} = \frac{K\,(P)^{0.924}\,(D)^{0.428}}{(d)^{0.206}\,(\rho)^{0.342}\,(L)^{0.838}} \quad (24)$$

Where K = $1.027 \times 10^{-5} = \frac{mm^2}{kgN}$

3.3 Teaching-learning-based optimization algorithm

Teaching-Learning based Optimization (TLBO) algorithm is a global optimization method originally developed by Rao et al. [23].TLBO is an optimization algorithm based on teaching and learning process in a classroom. The searching process consists of two phase, i.e. Teacher phase and Learner Phase. In teacher phase, learners first get knowledge from a teacher and then from other classmates in learner phase. In the entire population, the best solution is considered as the teacher (Xteacher). On the other hand, learners seek knowledge from the teacher in the teacher phase. In this phase, the teacher tries to improvise the results of other individuals (Xi) by increasing the mean results of the classroom (Xmean) towards his/her position Xteacher. In order to maintain uncertain features of the search, two randomly-generated parameters r and T_f are applied in update formula for the solution Xi as:

$$X_{new} = X_i + r(X_{teacher} - T_f * X_{mean})$$

Where r is a randomly selected number in the range of 0 and 1 and T_f is a teaching factor which can be either 1 or 2:

$$T_f = \text{round}\,[1 + \text{rand}(0,1)\{2-1\}]$$

Moreover, X_{new} and X_i are the new and existing solution of i.

In the learner phase, the learner attempt to increase their information by interacting with other learners. Therefore, an individual learns new knowledge if the other individuals have more knowledge compared to the other learner. Throughout this phase, the student Xi interacts randomly with another student Xj (where $i \neq j$) in order to improve his/her knowledge. In the case that if Xj is better than Xi (then $f(X_j) < f(X_i)$ for minimization problem), Xi is moved towards Xj. Otherwise it is moved away from Xj :

$X_{new} = X_i + r.(X_j - X_i)$ if $f(X_i) > f(X_j)$

$X_{new} = X_i + r.(X_i - X_j)$ if $f(X_i) < f(X_j)$

If the solution X_{new} is better, it is accepted in the population. The algorithm will continue until the termination condition is met.

3.4 Optimization of parameters of SFC through TLBO

Optimization performance of TLBO is determined by the Analyzed data and mathematical modeling as considered here..A computer code is developed using MATLAB R2013a for the parametric optimization in AWSJ machining process considering the Population size 12 and

Objective of using TLBO is to minimize the SFC given by the eq. 24.

Generation – 1

Table 3: Initial Population

P (Bar)	D (mm)	d (mm)	ρ (kg/m^3)	L (mm)	SFC
200	3.8	1.20	2500	17.4	0.0021
240	4.2	1.30	2600	17.5	0.0025
280	3.8	1.40	2700	17.6	0.0027
320	4.2	1.25	2800	17.7	0.0032
360	3.8	1.35	2900	17.8	0.0033
230	4.2	1.45	3000	17.9	0.0022
370	3.8	1.20	2400	17.9	0.0037
350	4.2	1.30	2470	17.8	0.0036
300	3.8	1.40	2550	17.7	0.0029
180	4.2	1.25	2630	17.6	0.0019
250	3.8	1.35	2750	17.5	0.0024
300	4.2	1.40	2850	17.4	0.0030

Table 4: Teacher Phase

P_{new} (Bar)	D_{new} (mm)	d_{new} (mm)	ρ_{new} (kg/m^3)	L_{new} (mm)	SFC_{new}
135.95	3.906	1.1695	2474	17.3685	0.0015
175.95	4.306	1.2695	2574	17.4685	0.0019
215.95	3.906	1.3695	2674	17.5685	0.0022
255.95	4.306	1.2195	2774	17.6685	0.0026
295.95	3.906	1.3195	2874	17.7685	0.0028
165.95	4.306	1.4195	2974	17.8685	0.0017
305.95	3.906	1.1695	2374	17.8685	0.0031
285.95	4.306	1.2695	2444	17.7685	0.0030
235.95	3.906	1.3695	2524	17.6685	0.0024
115.95	4.306	1.2195	2604	17.5685	0.0013
185.95	3.906	1.3195	2724	17.4685	0.0019
235.95	4.306	1.3695	2824	17.3685	0.0024

Table 4: Modified value after teacher phase

P_{mod} (Bar)	D_{mod} (mm)	d_{mod} (mm)	ρ_{mod} (kg/ m^3)	L_{mod} (mm)	SFC_{mod}
135.950	3.9060	1.1695	2474	17.3685	0.0015
175.950	4.3060	1.2695	2574	17.4685	0.0019
215.950	3.9060	1.3695	2674	17.5685	0.0022
255.950	4.3060	1.2195	2774	17.6685	0.0026
295.950	3.9060	1.3195	2874	17.7685	0.0028
165.950	4.3060	1.4195	2974	17.8685	0.0017
305.950	3.9060	1.1695	2374	17.8685	0.0031
285.950	4.3060	1.2695	2444	17.7685	0.0030
235.950	3.9060	1.3695	2524	17.6685	0.0024
115.950	4.3060	1.2195	2604	17.5685	0.0013
185.950	3.9060	1.3195	2724	17.4685	0.0019
235.950	4.3060	1.3695	2824	17.3685	0.0024

Table 5: Learner phase

P_{nbest} (Bar)	D_{nbest} (mm)	d_{nbest} (mm)	ρ_{nbest} (kg/ m^3)	L_{nbest} (mm)	SFC_{nbest}
123.35	4.1180	1.1910	2543	17.4945	0.0014
138.15	4.3060	1.2480	2590	17.5315	0.0015
152.95	4.1180	1.3050	2637	17.5685	0.0016
152.95	4.1180	1.3050	2637	17.5685	0.0018
182.55	4.1180	1.2765	2731	17.6425	0.0019
134.45	4.3060	1.3335	2778	17.6795	0.0014
186.25	4.1180	1.1910	2496	17.6795	0.0020
178.85	4.3060	1.2480	2529	17.6425	0.0019
160.35	4.1180	1.3050	2566	17.6055	0.0017
27.750	4.3060	1.2195	2514	17.5055	0.0004
141.85	4.1180	1.2765	2660	17.5315	0.0015
160.35	4.3060	1.3050	2707	17.4945	0.0017

Table 6: Modified value after learner phase

P_{mod} (Bar)	D_{mod} (mm)	d_{mod} (mm)	ρ_{mod} (kg/m^3)	L_{mod} (mm)	SFC_{mod}
123.350	4.1180	1.1910	2543	17.4945	0.0014
138.150	4.3060	1.2480	2590	17.5315	0.0015
152.950	4.1180	1.3050	2637	17.5685	0.0016
152.950	4.1180	1.3050	2637	17.5685	0.0018
182.550	4.1180	1.2765	2731	17.6425	0.0019
134.450	4.3060	1.3335	2778	17.6795	0.0014
186.250	4.1180	1.1910	2496	17.6795	0.0020
178.850	4.3060	1.2480	2529	17.6425	0.0019
160.350	4.1180	1.3050	2566	17.6055	0.0017
115.950	4.3060	1.2195	2604	17.5685	0.0013
141.850	4.1180	1.2765	2660	17.5315	0.0015
160.350	4.3060	1.3050	2707	17.4945	0.0017

Generation – 2

Modified values after learner phase of First generation are taken as Initial population for the Second generation and then same operations are performed and the best set of solution of optimum values of parameters for minimum value of SFC after second generation is given in the Table no. 8.

Table 8: Modified value after learner phase

P_{mod} (Bar)	D_{mod} (mm)	d_{mod} (mm)	ρ_{mod} (kg/m^3)	L_{mod} (mm)	SFC_{mod}
105.905	4.2645	1.2031	2555	17.4985	0.001197

4. RESULT AND DISCUSSION

Optimized values of parameters for minimum SFC are:

Inlet Operating Pressure Bar	105.95
Nozzle diameter mm	4.2645
Orifice diameter mm	1.2031
Density of Abrasive article	2555 kg/m^3
Focus length	17.4985 mm

The minimum value of SFC for optimized value of parameters is 0.001197.

4.1 Confirmation Analysis for optimum value

The confirmation analysis has performed at optimum value of parameters using commercially available pre-processor routine called GAMBIT. CFD Analysis has performed to obtain the value of SFC for optimized set of parameters and the Analyzed value of SFC is 0.001127 and it is closer to the predicted value.

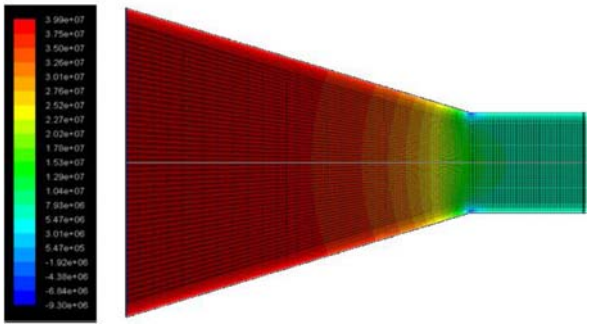

Fig. 5: Contours of static pressure (mixture) (Pascal) as per the present model.

5. CONCLUSION

The optimized value of SFC through TLBO is 0.001197 and it is closer to Analyzed value of SFC. In the present work, According to the structure of nozzle computational domain has been modeled using commercially available pre-processor routine called GAMBIT, and CFD Analysis has been performed in ANSYS (fluent) to obtain the values of SFC for different values of parameters. Based on the Analysis at the critical section of nozzle an empirical formula has been developed for nozzle geometry. TLBO algorithm has been used to optimize the parameters to minimize the SFC in AWSJ machining. To confirm the result CFD Analysis has been performed to obtain the value of SFC for optimized value of parameters.

References

[1] N. C. Markatos, "Modelling of two-phase transient flow and combustion of granular propellants." *International Journal of Multiphase flow, vol. 12, no. 6, pp. 913-933, 1986.*

[2] M. Hashish, Observation of wear of abrasive-waterjet nozzle materials, *Journal of Tribology* 116 (1994) 439-444.

[3] Fluent User's Guide, vol. 3, Fluent Incorporated Publishers,Lebanon, 1998.

[4] G. Hu, W. Zhu, T. Yu, and J. Yuan, "Numerical simulation and experimental study of liquid-solid two-phase flow in nozzle of DIA jet", *Proceedings of the IEEE International conference industrial informatics (INDIN 2008)*, Daejeon, Korea, July 13-16th 2008

[5] G. J. Brown, "Erosion prediction in slurry pipeline teejunctions," *Applied Mathematical Modelling, vol. 26, no. 2, pp. 155–170, 2002.*

[6] Nanduri M, Taggart DG, Kim TJ (2002), The effects of system and geometric parameters on abrasive waterjet nozzle wear. *Int J Mach Tools Manuf* 42: 615-623.

[7] J. Chahed, V. Roig, and L. Masbersnat, "Eulerian-eulerian two-fluid model for turbulent gas-liquid bubbly flows," *International Journal of Multiphase Flow*, vol. 29, no. 1, pp. 23–49, 2003.

[8] P.K. Mishra; Non-conventional machining, Narosa publishing house, Third reprint- 2005.

[9] H. Liu, J. Wang, N. Kelson, R. Brown, A study of abrasive waterjet characteristics by CFD simulation, Journal of Materials Processing Technology 153-154 (2004) 488-493.

[10] J. John RozarioJegaraj, N. Ramesh Babu, A strategy for efficient and quality cutting of material with abrasive waterjets considering the variation in orifice and focusing nozzle diameter, *Int. J. Mach. Tools Manuf.* 45 (12-13) (2005) 1443-1450.

[11] K. Maniadaki, T. Kestis, N. Bilalis, A. Antoniadis, A finite element-based model for pure water-jet process simulation, *Int. J. Adv Manuf. Technol.* (2007) 31: 933-940.

[12] B. S. Nie, J. Q. Meng, and Z. F. Ji, "Numerical simulationon flow field of pre-mixed abrasive water jet nozzle," in *Proceedingsof the Asia Simulation-7th International Conference on System Simulation and Scientific Computing (ICSC '08)*, pp.247–251, October 2008.

[13] D. S. Srinivasu,N.RameshBabu, A neuro-geneticapproach for selection of process parameters in abrasive waterjet cutting considering variation in diameter

of focusing nozzle, *in applied soft computing* 8 (2008) 809-819.

[14] T. Nguyen, D.K. Shanmugam, and J. Wang, " Effect of liquid properties on the stability of an abrasive waterjet" *International Journal of Machine Tools and Manufacture, vol, 48, no. 10, pp.1138-1147, 2008.*

[15] H.Z. Li, J. Wang, J.M. Fan, Analysis and modeling of particle velocities in micro-abrasive air jet, International Journals of Machine Tools & Manufacture 49 (2009) 850-858.

[16] N. Pi and N. Q. Tuan, "A study on nozzle wear modeling in abrasive waterjet cutting," a*dvanced Materials Research*, vol.76, pp. 345–350, 2009.

[17] M.G. Mostofa, K. Yong Kil, A. J. Hwan, computational fluid analysis of abrasive waterjet cutting head,*Journal of Mechanical Science and Technology* 24 (2010) 249-252.

[18] M. Zohoor, S.HadiNourian, Development of an algorithm for optimum control process to compensate the nozzle wear effect in cutting the hard and tough material abrasive water jet cutting process,*Int. J AdvManufTechnol* (2012) 61:1019-1028.

[19] Help documentation of 'GAMBIT 2.3.16' Software.

[20] D. Deepak, D. Anjaiah D, K. VasuudevaKaranth, and N. Yagnesh Sharma, CFD Simulation of flow in an Abrasive Water Suspension Jet: The Effect of Inlet Operating Pressure and Volume Fraction on Skin Friction and Exit Kinetic Energy, *Hindawi Publishing Corporation, Advance in Mechanical Engineering, Volume* 2012*, Article ID* 186430.

[21] Help documentation of 'Fluent 6.3.26' Software

[22] S. Anwar, D. Axinte and A.A Becker, Finite element modelling of abrasive waterjet milled footprints Faculty of Engineering, Department of Mechanical, Materials and Manufacturing Engineering, University of Nottingham, NG7 2RD, UK, Volume 213, Issue 2, February 2013, Pages 180–193.

[23] Rao, R.V., Savsani, V.J. & Vakharia, D.P. (2011).Teaching-learning-based optimization: A novel method for constrained mechanical design optimization problems. *Computer-Aided Design,* 43 (3), 303-315.

[24] Rao, R.V., Pawar, P.J. and Shankar, R., 2008. Multi-objective optimization of electrochemical machining process parameters using a particle swarm optimization algorithm.*Proceedings of the Institution of Mechanical Engineers, Journal of Engineering Manufacture*, 222, 949–958.

[25] MATLAB, user manual of MATLAB (2013).

[26] U. Anand and J. Katz, "Prevention of nozzle wears abrasive water suspension jet (AWSJ) using porous lubricated nozzle, *"Journal of Tribology, vol.125, no.1, pp.168-180,2003.*

[27] Deepak. D, Anjaiah D and Yagnesh Sharma, "Numerical analysis of flow through abrasive water suspension jet: the effect of abrasive grain size and jet diameter ratio on wall shear", *International Journal of Earth Sciences and Engineering*, Vol. 04, no 04 spl, pp. 78-83, ISSN 0974-5904.

[28] Rao, R.V., & Patel, V. (2012). An elitist teaching-learning-based optimization algorithm for solving complex constrained optimization problems. *International Journal of Industrial Engineering Computations*, 3(4), 535-560.

[29] M. J. Steinkamp, T. T. Clark, and F. H. Harlow, "Twopointdescription of two-fluid turbulent mixing-II. Numericalsolutions and comparisons with experiments," *InternationalJournal of Multiphase Flow, vol. 25, no. 4, pp. 639–682, 1999*.